

## THE EFFECT OF BALL MILLING ON THE MORPHOLOGY OF CUBIC BORON NITRIDE

A R Shashikala<sup>1a\*</sup>, Kothakula Keerthi<sup>2a</sup>, Ramesh C S<sup>3b</sup> and B S Sridhar<sup>4c</sup>

**Abstract:** Due to its attractive properties, cubic boron nitride (c-BN) finds extensive applications in mechanical and electronic industries. The conversion of micro c-BN to nano c-BN remarkably influences the properties. This study investigates the effect of ball milling on the morphological parameters. Boron nitride was subjected to different hours of ball milling process at different rotation speeds. The crystallite size of the c-BN was measured at different ball milling time intervals, and it is observed that after 100 hours, the crystallite size decreased to nano size. The ball milling was increased to 150-175 hours to get less than 100 nm size particles. The surface morphology and elemental analysis of the samples were done using SEM and EDX studies. EDX confirmed the presence of boron and nitrogen in the sample. SEM images indicated that the agglomerated morphology of c-BN particles with irregular shape. The cubic structure was confirmed from XRD studies. Thermogravimetric analysis (TGA) conducted to determine the samples' thermal stability indicated that weight loss was observed for temperatures up to 700°C. There was no significant weight loss at a higher temperature. Stronger reflectance was observed with increased ball milling time in UV-Visible DSR studies.

**Keywords:** c-BN, ball-milling, XRD, crystallite size, thermogravimetric analysis, uv-visible DSR

### 1. Introduction

Boron nitride is an iso-electronic with carbon because boron and nitrogen are present side by side individually to the carbon atom in the periodic table [1]. BN can be synthesized in four polymorphic structures viz hexagonal BN (h-BN), rhombohedral BN (r-BN), wurtzite- BN (w-BN) and cubic BN (c-BN) [2]. h-BN has delocalized pi orbital with sp<sup>2</sup> hybridization. Hexagonal Boron Nitride exhibits the same crystal structure-like graphite [3]. It finds extensive application as an additive in cosmetic products, used as effective lubricant when added with other alloys, plastics, resins, etc. [4]. A combination of BN with CNTs is prone to increase applications of h-BN in electronic devices and gas storage materials [5].

In r-BN boron and nitrogen are packed with four-membered rings of layers. No four-layer coincidence occurred, but a displacement was seen on every fourth layer and repeated at the first layer. It exhibits sp<sup>2</sup> hybridization, where three covalent bonds connect each other with their neighboring atoms [6].

Boron and nitrogen atoms in w-BN have 6-membered rings. The rings between layers are in a boat configuration. However, the c-BN layers are in a chair configuration. Recent studies indicate that w-BN is harder than other borides but softer than c-BN [7].

On the other hand, c-BN is extremely hard, close to a diamond's hardness. It exhibits a single crystal phase and sp<sup>3</sup> hybridization similar to diamond [2]. As a semiconductor, it shows a wide band gap, has good optical properties, high thermal conductivity and is chemically inert [8-10]. c-BN shows good transmittance with a wide band gap and spectral range from a UV to Visible [11-14]. c-BN can be doped with p- or n-type impurities [15, 16] to improve its band gap and thermal stability. Due to its wide band gap and thermal stability, it finds applications in high-temperature power electronic instruments, unlike diamond [17]. c-BN can be used in cutting tools and optical instruments like UV detectors and emitters [18-20]. It is insoluble at room temperature but is still used as abrasive because it has high-temperature solubility with nickel, iron and its alloys [21].

Nano c-BN can be obtained by a simple top-down process. Ball milling is a top-down process that synthesizes various nanoparticles like metal oxides, zeolites, carbon materials, and metal frameworks [22, 23]. Nanoparticles obtained from the ball milling process have wide applications in fuel cells, electronic devices, drug delivery and catalysis [24]. Ball-milling increases the surface area and changes the chemical functionality and morphology. Ball-milling in the presence of hydrogen, ammonia, or sodium hydroxide leads to forming ex-foliated boron nitride

#### Authors information:

<sup>a</sup>Department of Chemistry, Presidency University, Itgalpura, Rajankunte, Yelahanka, Bangalore, INDIA-560064. E-mail: aarudirs@gmail.com<sup>1</sup>; kothakulakeerthy@gmail.com<sup>2</sup>

<sup>b</sup>Department of Mechanical Engineering, Presidency University, Itgalpura, Rajankunte, Yelahanka, Bangalore, INDIA-560064. E-mail:

crramesh@presidencyuniversity.in<sup>3</sup>

<sup>c</sup>MSRIT, Department of Mechanical Engineering, Bangalore, INDIA-560054. E-mail: sridharbs@msrit.edu<sup>4</sup>

\*Corresponding Author: aarudirs@gmail.com

Received: January 11, 2022

Accepted: October 4, 2022

Published: October 31, 2023

with hydroxyl and amino groups on the surface [25-28].

In this work, nano c-BN was prepared by the ball-milling process. We studied the effect of ball-milling time and rotational speed on the morphology, crystal structure, particle size and thermal stability.

## 2. Materials and Methods

Commercial cubic boron nitride (c-BN) with a particle size of 2 μm was used for the ball milling process. The sample was subjected to different ball-milling time intervals of up to 175 hours and carried out at 50 and 100 rpm.

Ball milling was conducted using the Delta Power Controls Planetary Ball mill with stainless steel balls of 12 grams weight and vials. The impact force jar was stationary and revolved in a planetary orbit. The ball milling was carried out at different rotations per minute (rpm) and at different period without any power interruption.

The samples' elemental analysis was carried out with EDX using the Link Ge Energy Dispersive Spectrometer combined with a Noran Scientific analyzer, Model TN5500, USA, which provides the spatial resolution for compositional analysis and is limited to 1-micrometer diameter on flat specimens.

The Scanning Electron Microscope TESCAN-VEGA3 LMU was used to study the microstructure and surface morphology at different ball milling times and rotational speeds. The XRD analysis of the milled samples was carried out using an X-ray diffractometer, Philips, PW 1140/90, USA, equipped with Ni filter and Cu K radiation [29]. Double beam UV-visible spectrophotometer model UV 2600 with 200 to 800 nm spectral band was used to measure samples reflectance at different ball milling times. The thermogravimetric analysis was studied using the NETZSCH's STA 449 F5 Jupiter Simultaneous Thermal Analyzer TGA/DSR.

## 3. Results and Discussion

Table 1 depicts the EDX-elemental composition of c-BN after different grinding duration at 50 rpm. Iron appeared as an impurity when the grinding time was increased to 175 hours because of the stainless steel balls used in the ball milling process. The balls were coated with Teflon and subjected to 175 hours of grinding to overcome this. Table 1 shows the elemental composition of the nano c-BN powder at 175 hours of ball milling before and after coating the balls with Teflon. Boron

concentration decreased with increased ball milling time, which may be due to the diffusion of boron into steel balls during ball milling. The diffusion increased at higher rpm, which may be due to increased temperature with increased ball milling speed and diffusion at higher temperatures [30, 31].

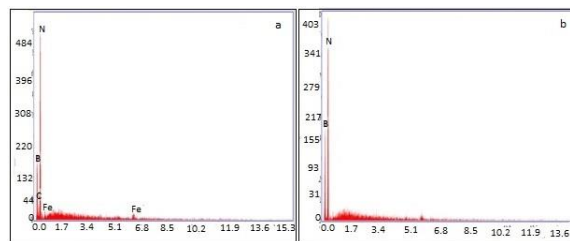


Figure 1. EDAX images of nano c-BN at 175 hours: a) before Teflon coating b) after Teflon coating

Table 1. Elemental composition of the nano c-BN powder at different grinding times at 50 rpm

Time(hrs)	Element	Weight (%)
100	B	50.45
	N	49.55
125	B	48.45
	N	51.04
150	B	48.04
	N	51.66
	B	43.98
175 (before coating the balls with Teflon)	N	54.67
	C	0.41
	Fe	0.26
175 (after coating the balls with Teflon)	B	48.09
	N	51.91

Table 2 shows the presence of iron, chromium, nickel, oxygen, boron, and nitrogen due to using steel balls for grinding. For all further characterization, nano powder obtained at 50 rpm and 175 hours of ball milling with Teflon-coated balls was used as it is free from other impurities.

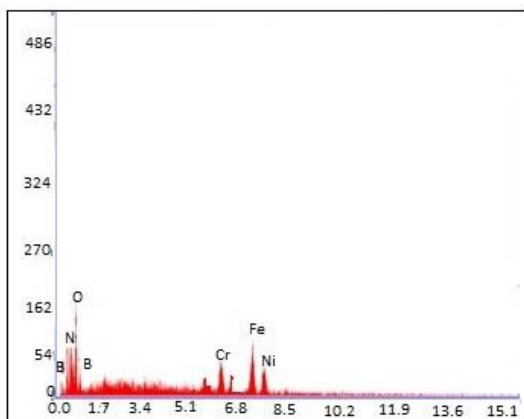


Figure 2. EDAX Image of nano c-BN at 100 rpm

Table 2. Elemental composition of nano c-BN powder at 100 rpm

Time(hrs)	Element	Weight (%)
100	B	46.08
	N	26.23
	Fe	12.68
	Cr	3.65
	O	10.07
	Ni	1.27

Figure 3 shows the XRD images of c-BN at different grinding times. There are four characteristic peaks corresponding to (111), (200), (220) and (311) at 43.6°, 50.9°, 74° and 90°, respectively. The diffraction peaks were only slightly weakened with increased ball milling time due to c-BN's superior hardness. This is similar to the phenomenon reported by Zia and Li [32]. The intensity of (200) peak was decreased to a maximum extent compared to other peaks at 175 hours of ball milling. The c-BN crystallite size decreased with increased ball milling time. Its size decreased from 400 nm at 50 hours of ball milling to 66 nm at 175 hours.

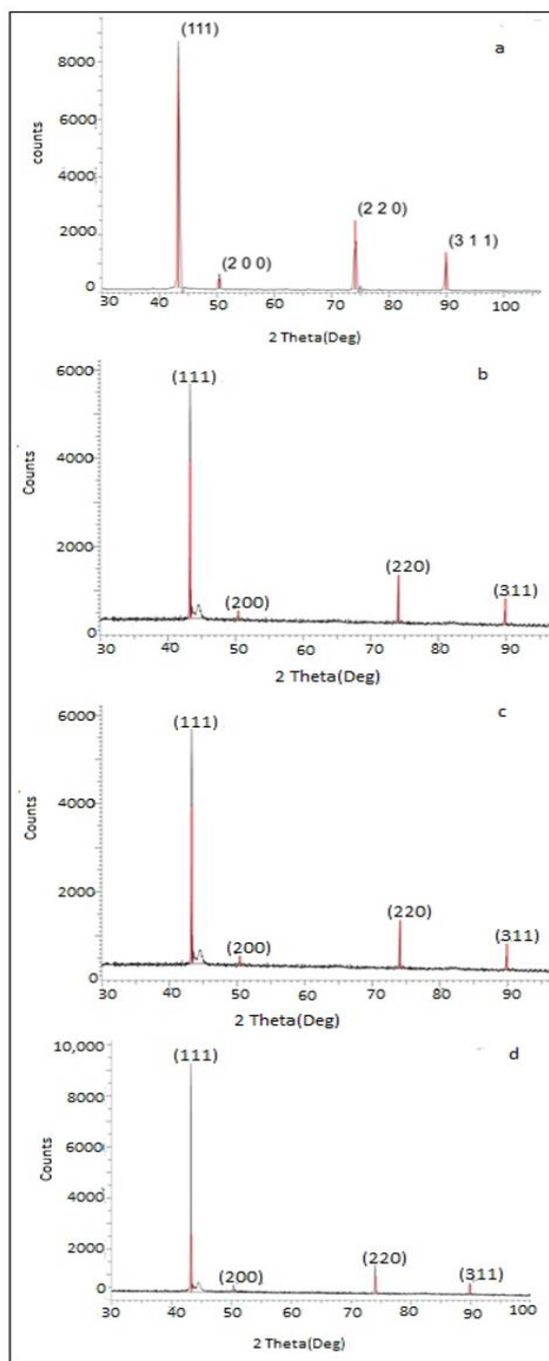


Figure 3. XRD images of c-BN at 50 rpm and different grinding times:

- a)100 hrs.
- b)125 hrs.
- c)150 hrs.
- d)175 hrs.

Figure 4 depicts an XRD image of nano c-BN obtained at 100 hours of ball-milling and 100 rpm speed. The peak intensity decreased and disappeared at 50.9° and 90° with increased speed.

Figure 5 shows the effect of different rotational speeds on the c-BN's crystallite size. Initially, the experiments were conducted at 50 rpm at different grinding times of up to 175 hours. The crystallite size decreased to ~66 nm from 2 μm. The size remained almost constant after 175 hours of ball milling. Experiments were also conducted at 100 rpm. Increasing the rpm decreased the crystallite size; at 100 hours and 50 rpm, the size decreased to less than 60 nm from 125 nm.

Figure 6 displays the scanning electron micrograph of c-BN powder at different ball milling times. The micrographs magnification was kept constant. The specimen was found to have an irregular shape with few agglomerates. Increasing the ball milling time caused the c-BN nanoparticles to have irregular morphologies with sizes that ranged from 57 to 78 nm.

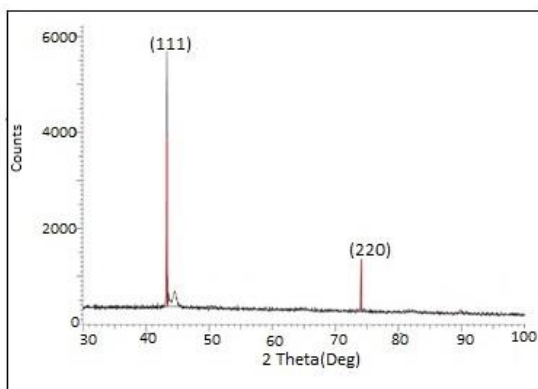


Figure 4. XRD images of c-BN at different grinding times with 100 rpm

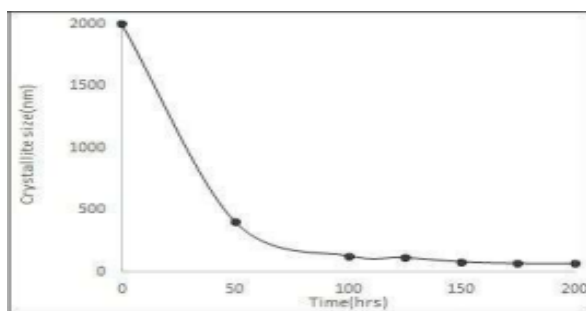


Figure 5. Effect of ball milling on the crystallite size of c-BN at 50 rpm

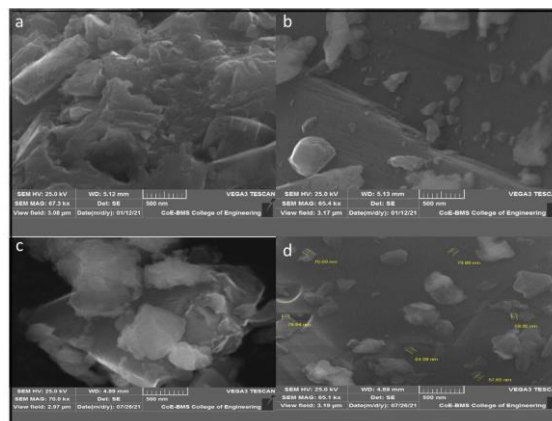


Figure 6. SEM images of c-BN at different ball milling times:

- a) 100 hrs.
- b) 125 hrs.
- c) 150 hrs. and
- d) 175 hrs.

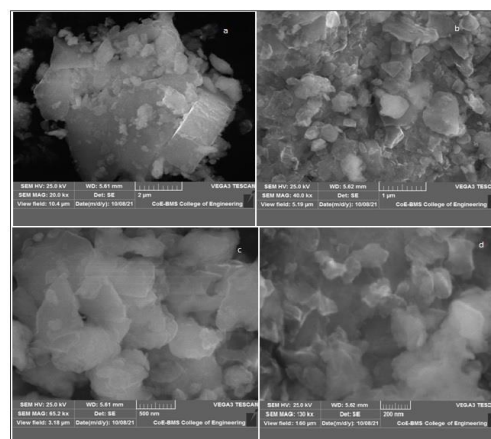
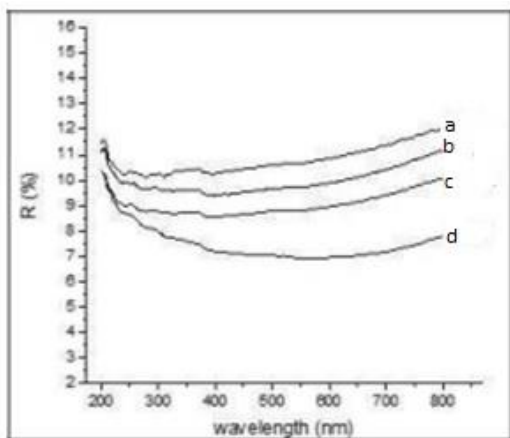


Figure 7. SEM images of c-BN at 100 rpm (100 hrs.) at different magnifications: a) 2 μm b) 1 μm c) 500 nm d) 200 nm.

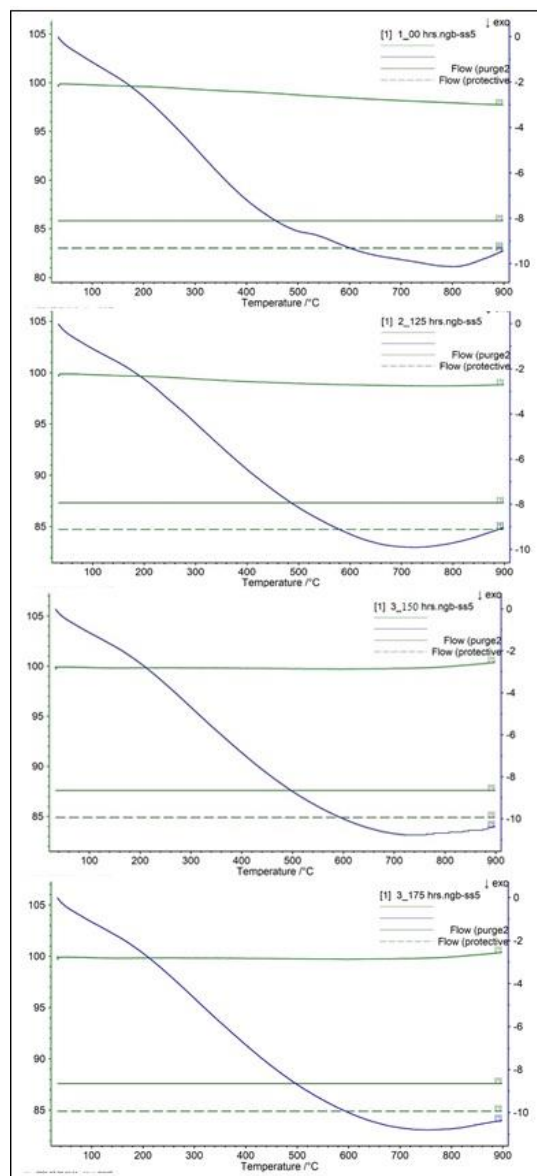
Figure 7 depicts SEM images of nano c-BN obtained at 100 hours at 100 rpm at different magnifications. At 100 rpm, c-BN consisted of nano-sized amorphous particles with few nodular lumps. The particle size ranged from 60 to 70 nm.

Figure 8 shows the UV-visible DSR spectra of c-BN at different ball milling times. All samples showed UV reflectance in the visible region. The incident light absorption occurred in the 200–800 nm wavelength range. Around 7-12% of reflection is in the longer wavelength region. Overall, reflectance intensity was remarkably enhanced with increased time. Stronger reflectance was observed with increasing ball milling time compared to the micro-sized c-BN.



**Figure 8.** UV-visible DSR spectra of c-BN at different ball milling time:  
 a) 0 hrs b) 50 hrs c) 125 hrs d) 175 hrs

The thermal stability test was conducted to study the effect of ball milling time on the degradation temperature of c-BN. Figure 9 shows the Thermogravimetric analysis. The TGA graphs are similar for all samples. The weight loss occurred for all samples at room temperature up to 700°C except for the sample obtained at 175 hours of ball milling. The weight loss may be attributed to the increased surface area of the ball-milled sample. The weight loss is as high as 3% in the 100-hour ball-milled sample. The weight loss slightly decreased as the grinding time increased, as seen in the 150- and 175-hour ball-milled sample. No significant weight loss was observed for all samples after 700°C. After the TGA test, ash was collected for all samples, and the amount of ash formed at higher ball milling time was significantly less than that for 100 hours of ball milling.



**Figure 9.** Thermogravimetric analysis of c-BN

## 4. Conclusion

Nano c-BN was obtained through a simple, eco-friendly ball milling process at different rotational speeds. Effect of ball milling time on morphology and crystallite size was studied. Nano c-BN obtained at 150 to 175 hours of ball milling at 50 rpm were used for the characterization studies. XRD data revealed that increasing ball milling time decreased the peak intensity, and a few peaks disappeared with increased rpm. c-BN nanoparticles were found to have irregular shapes with sizes ranging from 57 to 78 nm. Stronger reflectance was observed with increased ball milling time in the DSR spectra. There was weight loss for all samples at room temperature up to 700°C in the TGA studies. No significant weight loss was observed for all samples after 700°C.

## 6. References

- Arkundato A., Hasan M., Purwandari E., Pramutadi A., & Aziz F., "Temperature dependence diffusion coefficients of iron, boron and iron-boron calculated by molecular dynamics method" *J. Phys.: Conf. Ser.* (2019) 1170. doi:10.1088/1742-6596/1170/1/012008.
- Arkundato A., Su'ud Z., Abdullah M., & Widayani "Inhibition of high corrosion in high temperature stagnant liquid lead: A molecular dynamics study." *AIP Conf Proc* 1244 (2010) 136. doi.org/10.1088/1742-6596/1170/1/012008.
- Arya S. P. S., & D'Amico A., "Preparation, properties and applications of boron nitride thin films". *Thin Solid Films*, 157, (1988), 267–282. doi.org/10.1016/0040-6090(88)90008-9
- Bass J. D., Solovyov A., Pascall A. J., Katz A., & Am J. "Acid-Base Bifunctional and Di-electric Outer-Sphere Effects in Heterogeneous Catalysis: A Comparative Investigation of Model Primary Amine Catalysis". *Chem. Soc.*, 128, (2016), 3737–3747. doi.org/10.1007/s10934-011-9546-x.
- Brazhkin, Vadim V.; Solozhenko, Vladimir L. "Myths about new ultrahard phases: Why materials that are significantly superior to diamond in elastic moduli and hardness are impossible". *J. Appl. Phys.* 13, (2019), 125. doi.org/10.1063/1.5082739.
- Bennett T. D., & Cheetham A. K., "Amorphous Metal-Organic frameworks". *Acc. Chem. Res.* 47, (2014), 1555–1562.
- Davis R. F., "III-V nitrides for electronic and optoelectronic applications". *Proc. IEEE*, 79, (1991), 702. www.lib.ncsu.edu/resolver/1840.2/610
- DeVries C., "Recent advances in grinding". *Research Conference Proceedings*, 25, (1972), 178. doi.org/10.1007/978-1-4615-8300-410.
- Gielisse P. J., Mitra S. S., Plend J. N., Griffis R. D., Mansur L. C., Marshall R. & Pascoe E. A., "Lattice infrared spectra of Boron Nitride and Boron mono phosphide". *Phys. Rev.*, 155, (1967), 1039–1046. doi.org/10.1103/PhysRev.155.1039.
- Ishii T., Sato T., Sekikawa Y., Iwata M., "Growth of whiskers of hexagonal Boron Nitride", *Crystal Growth*, 52, (1981), 285–289. doi.org/10.1016/0022-0248(81)90206-2.
- Kester D. J., & R. Messier., "Mechanism of nucleation and growth of cubic-Boron Nitride thin films". *J. Appl. Phys.*, 72, (1992), 504–513. doi.org/10.1016/S1468-6996(01)00004-3.
- Laurence Vel, Gerard Demazeau and Jean Etourneau "Cubic boron nitride: synthesis, physicochemical properties and applications". *Mater. Sci. Eng. B* (1991) 149–164. doi.org/10.1016/0921-5107(91)90121-B.
- Lee D., Lee B., Park K. H., Ryu H. J., Jeon S., & Hong S. H., "Scalable exfoliation process for highly soluble boron nitride nanoplatelets by hydroxide assisted ball-milling". *Nano Lett.*, 15, (2015), 1238–1244. doi.org/10.1038/srep07288.
- Liu L., Xiong Z., Hu D., Wu G., Liu B., & Chen P., "Solid Exfoliation of Hexagonal Boron Nitride Crystals for the Synthesis of Few-layer Boron Nitride Nanosheets". *Chem. Lett.*, 42, (2013), 1415–1416. doi.org/10.1016/j.carbon.2014.10.008.
- Lu C. J., & Li Z. Q., "Thermodynamic aspects of nano structured Ti<sub>5</sub>Si<sub>3</sub> formation during mechanical alloying and its characterization". *J. Alloy. Compd.* 395, (2005) 88. doi.org/10.1007/s12034-012-0298-2.
- Lu M., Bousetta A., Sukach R., Bensaoula A., Waters K., Eipers-Smith K. & Schultz J. A., "Growth of c-BN on Si (100) by neutralized nitrogen ion bombardment". *Appl. Phys. Lett.*, 64, (1994), 1514–1516.
- Mishima O., Era K., Tanaka J., & Yamoka S., "Observation of a hexagonal BN surface layer on the cubic BN film grown by dual ion beam sputter deposition". *Appl. Phys. Lett.*, 53, (1988), 962–964. doi.org/10.1063/1.118402.
- Orellana-Tavara C., Baxter E. F., Tian T., Bennett T. D., Slater N. K. H., Cheetham A. K., & Fairen-Jimenez D., "Amorphous metal-organic frameworks for drug delivery". *Chem. Commun.*, 51, (2015), 13878–13881. doi.org/10.1039/C5CC05237H.

- Pouch J. J., & Alterovitz S. A., "Review of synthesis and properties of cubic boron nitride (c-BN) thin films". Brookfield, Trans Tech Publications. Proc. Mater. Sci. Forum, 54/55, (1990), 313–328. doi.org/10.1016/S0927-796X(97)00009-0.
- Reddy L. M., Srivastava A., & Gowda S. R., et al., "Synthesis of nitrogen-doped graphene films for lithium battery application," ACS Nano, 4, (2010) 6337–6342. doi.org/10.1021/nn101926g.
- Song L., Ci L., Lu H., Sorokin P. B., Jin C., Ni J., Kvashnin A. G., Kvashnin D. G., Lou J., Yakobson B. I. & Ajayan P. M., "Large Scale Growth and Characterization of Atomic Hexagonal Boron Nitride Layers." Nano Letters, 10, (2010), 3209–3215. doi.org/10.4236/jct.2013.46A2001.
- Shashikala, A R.; Mayanna, S M.; Sharma, A. Studies and characterization of electroless Ni–Cr – Palloy coating. Trans IMF, (2007), 85, 6, 320324. doi.org/10.1179/174591907X246483.
- Shashikala, A. R.; Sridhar, B, S. Codeposition of electroless Ni–P/ZnO nano composites and evaluation of corrosion resistance of the coatings. Materials Today: Proceedings, (2021), 45, 4, 3837–3840. doi.org/10.1016/j.matpr.2020.05.447.
- Todd R. H., Allen D. K., & Alting L., "Synthesis and preparation of mono-layer h-BN nano powders by using a combination of CVD method with iso-propanol- assisted exfoliation process". Manufacturing Processes Reference Guide, Industrial Press Inc., 55. N.Y. (1994), 43–48. doi.org/10.1007/s11106-017-9836-1.
- Vell., Demazeau G., & Etourneau J., "Cubic-boron nitride: synthesis, physicochemical properties and applications". Mater. Sci. Eng. B, 10, (1991), 149–164. doi.org/10.1016/0921-5107(91)90121-B.
- Wada T., & Yamashita N., "Cross-sectional transmission electron microscopy observations of c-BN films deposited in Si by ion- beam-assisted deposition". J. Vac. Sci. Technol. A, 10, (1992), 515–520. doi.org/10.1016/0040-6090(94)90297-6.
- Wang P., Orimo S., Matsushima T., Fujii H., & Majer G., "Synthesis of boron nitride nano fibers and measurement of their hydrogen uptake capacity". Appl. Phys. Lett., 80, (2002), 318–320. doi.org/10.1016/S0008-6223(03)00302-6.
- Wentorf R. H., Jr: "Preparation of semiconducting Cubic Boron Nitride". J. Chem. Phys., 36, (1962), 1990–1991. doi.org/10.1063/1.1732816.
- Xia Z. P., & Li Etourneau Z. Q. "Structural evolution of hexagonal BN and cubic BN during ballmilling" J. Alloy. Compd. 43(2007)170-173. doi.org/10.1016/j.jallcom.2006.06.100.
- Xia Z. P., Li Z. Q., Lu C. J., Zhang B., & Zhou Y., "Structural evolution of Al/BN mixture during mechanical alloying". J. Alloy. Compd. 399, (2005), 139. doi.org/10.1016/j.jallcom.2005.03.087.
- Zhi C. Y., Bando Y., & Tang C. C, et al., "Large scale fabrication of boron nitride nanosheets and their utilization in polymeric composites with improved thermal and mechanical properties," Adv. Mater., 21, (2009) 2889–2893. doi.org/10.1002/adma.200900323.